Characterization of a novel adeno-associated viral vector with preferential oligodendrocyte tropism

SK Powell[1], **N Khan**[1,6], **CL Parker**[1,7], **RJ Samulski**[1,2], **G Matsushima**[3], **SJ Gray**[1,4,8], and **TJ McCown**[1,5,8]

[1]Gene Therapy Center, Chapel Hill, NC, USA

[2]Department of Pharmacology, Chapel Hill, NC, USA

[3]Department of Microbiology and Immunology, Chapel Hill, NC, USA

[4]Department of Ophtalmology, Chapel Hill, NC, USA

[5]Department of Psychiatry, University of North Carolina, Chapel Hill, NC, USA

Abstract

No adeno-associated virus (AAV) capsid has been described in the literature to exhibit a primary oligodendrocyte tropism when a constitutive promoter drives gene expression, which is a significant barrier for efficient *in vivo* oligodendrocyte gene transfer. The vast majority of AAV vectors, such as AAV1, 2, 5, 6, 8 or 9, exhibit a dominant neuronal tropism in the central nervous system. However, a novel AAV capsid (Olig001) generated using capsid shuffling and directed evolution was recovered after rat intravenous delivery and subsequent capsid clone rescue, which exhibited a > 95% tropism for striatal oligodendrocytes after rat intracranial infusion where a constitutive promoter drove gene expression. Olig001 contains a chimeric mixture of AAV1, 2, 6, 8 and 9, but unlike these parental serotypes after intravenous administration Olig001 has very low affinity for peripheral organs, especially the liver. Furthermore, in mixed glial cell cultures, Olig001 exhibits a 9-fold greater binding when compared with AAV8. This novel oligodendrocyte-preferring AAV vector exhibits characteristics that are a marked departure from previously described AAV serotypes.

INTRODUCTION

Adeno-associated virus (AAV) vectors occupy a prominent position in gene transfer studies, where in the central nervous system (CNS) AAV vectors support long-term, non-toxic gene expression for up to 8 years in non-human primates.[1–3] These favorable properties have led

CONFLICT OF INTEREST

The remaining authors declare no conflict of interest.

to a number of ongoing phase I clinical studies focused upon Parkinson's disease, Alzheimer's disease and Canavans, yet to date, no serious adverse effects have been attributed to the AAV vectors.[4–6] The AAV serotypes most commonly used for CNS applications include AAV1, AAV2, AAV4, AAV5, AAV6, AAV8 and AAV9. Previously, AAV2 studies have dominated both preclinical and present clinical investigations, but recent discoveries of numerous distinct AAV serotypes have significantly expanded the transduction properties within the CNS.[7–10] For example, AAV8 and AAV5 transduce a significantly greater area of the CNS in comparison with AAV2, whereas AAV9 can cross the blood–brain barrier and transduce both neurons and astrocytes after intravenous administration.[7,10–11] Although these quantitative differences represent significant changes in the CNS transduction, very few differences exist in the cellular tropism, when a constitutive promoter drives gene expression. For example, after direct CNS infusion, almost all of the known AAV serotypes exhibit a dominant neuronal tropism, even across such diverse serotypes as AAV1, AAV2, AAV6, AAV8, AAV9, rh8, rh10, hu32 and hu37.[7,12–14] Some AAV capsids exhibit a weak tropism for oligodendrocytes when a cell-specific promoter drives expression (myelin basic protein). However, the overall transduction of oligodendrocytes is still low.[15–16] Despite the fact that many of these serotypes utilize different methods of cellular entry and intracellular trafficking, all of these diverse serotypes exhibit a dominant neuronal tropism.[7,10,12–13] The only exception is AAV4, which transduces ependymal cells, but not neurons, astrocytes, microglia or oligodendrocytes.[8] Similarly, this pervasive neuronal tropism also extends to numerous shuffled AAV capsid chimeras that were recovered in a previous study.[17] Clearly, substantial neuronal tropism appears to be a central feature across widely diverse AAV capsid structures.

The AAV capsids have nine variable regions surrounded by conserved regions where the variable regions form loops and clusters on the exterior of the capsid.[18–19] The unique topology of the AAV capsid confers cellular tropism by differential receptor binding. The first step of AAV transduction entails AAV binding to a primary receptor and co-receptor on the cell surface.[18] After cellular uptake into endosomes, AAV subsequently escapes from the endosome/lysosome and traffics to the perinuclear compartment.[20] These latter processes involve VP1- and VP2-specific portions of the capsid that contain acidification-responsive phospholipase domains and the nuclear localization signal.[20] Upon nuclear entry, the AAV virion uncoats, followed by AAV genome second-strand synthesis and, finally, transgene expression.[20] The present studies characterize a novel AAV vector generated from capsid shuffling and directed evolution that preferentially targets oligodendrocytes following intracranial injection into the striatum. Further, it shows increased extracellular binding to oligodendrocytes *in vitro* suggesting that the increased oligodendrocyte tropism is a result of external receptor interactions rather than downstream intracellular events.

RESULTS AND DISCUSSION

Identification of an oligodendrocyte-preferring AAV capsid

A shuffled AAV capsid library was created as described,[17] using the following parent capsids as starting material: AAV1, AAV2, AAV2i8,[21] AAV2.5,[22] AAV6, AAV8, AAV9, AAV9.47,[23] AAVrh10 and capsids recovered from unrelated ongoing shuffling projects. The

shuffled AAV capsid library was administered intravenously to a Sprague–Dawley rat 2 weeks after unilateral striatal administration of 6-hydroxy-dopamine (6-OHDA), and 3 days later AAV clones were recovered by PCR from dissociated striatal cells. The model creates a unique selective pressure on AAV, because 6-OHDA causes dopamine containing nerve terminals to degenerate, which leads to oligodendrocyte precursor cell infiltration.[24,25] Surprisingly, 10 of 10 selected clones had highly similar, if not identical sequences. Even with a second round of capsid shuffling, library administration and clone selection, 12 out of 12 clones had almost identical sequences, similar to the first round (Figure 1a). When the chimeric virus (named Olig001) was administered intravenously to unilateral 6-OHDA-treated rats, 2 weeks later immunohistochemistry revealed only a few green fluorescent protein (GFP)-positive neurons in the ipsilateral striatum and a sparse number of oligodendrocyte-like cells (data not shown). In marked contrast, 2 weeks after a striatal infusion of the Olig001 clone into naïve rats, oligodendrocytes comprised the vast majority of the transduced cells, even though GFP expression was driven by the constitutive chicken beta actin promoter (CBh) promoter (Figure 1).[26] The Olig001 capsid DNA sequence is shown in Figure 2, and a multiple protein alignment of Olig001 and its parental serotypes is shown in Figure 3. GFP-positive cells exhibited the typical oligodendrocyte morphology with clear labeling of myelin in the patch component of the striatal patch/matrix (Figure 1b). Furthermore, GFP-positive cells did not co-localize with glial fibrillary acidic protein, an astrocyte marker (Figure 1c), and < 5% of the GFP-positive cells co-localized with NeuN, a neuronal marker (Figure 1d). GFP-positive cells exhibit the typical morphology of striatal oligodendrocytes and co-localize with two oligodendrocyte markers, Olig2 (Figure 1e–g) and myelin basic protein (Figure 1h–j). Thus, almost all of the GFP-positive cells (> 95%) were oligodendrocytes with only a few neurons and no GFP-positive astrocytes or microglia.

These studies generated a novel chimeric AAV capsid variant with a preferential *in vivo* tropism for oligodendrocytes, a finding that represents a major departure from the normal neuronal tropism indicative of the parental AAV serotypes, except AAV4. AAV8 and AAV9 exhibit a dominant neuronal tropism after direct injection into the rodent striatum[9,13,16,27] as well as in other brain structures.[12,28,29] Past studies have described the ability of AAV2 or AAV8 to transduce oligodendrocytes at a low efficiency, but these studies required the use of oligodendrocyte-specific promoters to prevent expression in neurons, the preferred cell type for these vectors.[15,16] In contrast, using a ubiquitous promoter Olig001 has the ability to efficiently and preferentially transduce oligodendrocytes following intracranial administration. Thus, in the striatum Olig001 exhibits a preferred tropism for oligodendrocytes and low tropism for neurons, which is distinct from any previously reported AAV capsid.

Olig001 is detargeted from peripheral tissues

Given that the selection process involved intravenous administration of the capsid library, we sought to characterize the biodistribution of Olig001 in wild-type rodents compared with AAV8, the most represented AAV serotype in Olig001. Adult female C57Bl/6 mice received intravenous administration of equal amounts of either virus (5×10^{10} vg per mouse). Ten days later, organs were harvested, and the biodistribution was quantified by qPCR of the CBh-GFP transgene of Olig001-CBh-GFP (white bars) and AAV8-CBh-GFP (gray bars)

(Figure 4). The biodistribution of Olig001 was significantly reduced in all peripheral organs tested compared with AAV8, especially in the liver. The biodistribution of Olig001 indicates that it is not able to cross the blood–brain barrier, which was confirmed by a lack of GFP-positive staining in the brain by immunohistochemistry (data not shown). The peripheral tissue biodistribution profile of Olig001 is reduced in comparison with AAV1, AAV5 and AAV6 also.[30] Again, these data indicate that Olig001 has a highly divergent tropism from other AAV serotypes outside the CNS.

In vitro binding data

We performed an *in vitro* binding experiment using mixed glial cell cultures to better quantify the cell binding difference between Olig001 and AAV8, the most prominent parental serotype in Olig001. Mixed glial cell cultures were incubated with an equivalent amount of each virus, packaged with CBh-GFP transgene, for 1 h at 4 °C. This procedure allows vector binding to the cell surface, but prevents internalization.[31] After 1 h, the cells were washed with phosphate-buffered saline (PBS) to remove any unbound vector, then the cells were collected and total DNA was isolated from the cells. The amount of vector bound to cells was quantified by qPCR for GFP and normalized to mouse genomic LaminB2 (Figure 5a). Consistent with our *in vivo* results, Olig001 bound to the mixed glial cell population 9-fold more than AAV8. The proportion of oligodendrocytes in our mixed glial cell cultures were quantified by O4-positive staining of sister plates treated with AAV8 and Olig001 virus (Figure 5b). The AAV8-treated sister plate contained 89% O4-positive cells and the Olig001-treated sister plate contained 86% O4-positive cells indicating that the majority of the cells are oligodendrocytes and present in a similar percentage between the two conditions. Therefore, our *in vitro* data agrees with the observed *in vivo* tropism data of Olig001. These results indicate that *in vitro* Olig001 has a greater binding affinity for glial cell surface receptors than AAV8.

In total, our data describes a unique AAV vector with preferential oligodendrocyte tropism within the CNS and clear detargeting from peripheral tissues when intravenously injected. Thus, the Olig001 vector could be useful for *in vivo* and *in vitro* research applications requiring gene transfer to oligodendrocytes, which are typically refractory to efficient chemical transfection or vector-mediated transduction. Moreover, the ability to efficiently target oligodendrocytes *in vivo* could advance therapeutic strategies for demyelinating diseases such as Canavan disease or Krabbe disease.

MATERIALS AND METHODS

AAV capsid DNA shuffling and *in vivo* clone rescue

A shuffled AAV capsid was created as described[17] using the following parent capsids as starting material: AAV1, AAV2, AAV2i8,[21] AAV2.5,[22] AAV6, AAV8, AAV9, AAV9.47,[23] AAVrh10 and capsids recovered from unrelated ongoing shuffling projects.[32] The shuffled library was injected intravenously into rats that previously received a striatal 6-OHDA treatment. Three days later, the rats were killed and striatal cells were mechanically dissociated. DNA was recovered from neuron-enriched samples using the Qiagen DNeasy blood and tissue kit (Venlo, Netherlands) and subsequently concentrated by ethanol

precipitation. Intact capsid library sequences were recovered by PCR using a high-fidelity polymerase, Pfu Ultra II (Agilent, Santa Clara, CA, USA), with primers SwaICapUP 5′-GCGAATGATTTAAATCAGGTATGGCTGC-3′ and P4ext 5′-AAGCTCTAGACGGACACCAAAGTTCAACT-3′. A subsequent error-prone PCR step was employed to further diversify the library between rounds. Cloning and library amplification between selection rounds was carried out as previously described.[17] A total of two rounds of selection were performed. Recovered clones after each round were subcloned into rAAV pXR2 backbones and SSV9 replication-competent backbones and sequenced.

AAV vector production

Recombinant AAVs were produced using a triple plasmid transfection method in HEK293 cells, followed by iodixanol gradient centrifugation and ion-exchange chromatography, as previously described.[33] All AAV vectors were packaged with a self-complementary genome with enhanced GFP under the control of a cytomegalovirus enhancer, miniature CBh chicken beta-actin hybrid and minute virus of mice intron.[26] Peak fractions were dialyzed in PBS with 5% sorbitol, and NaCl added to a final concentration of 350 mm NaCl. Viral titers were obtained via qPCR (see below).

qPCR for biodistribution studies and viral titer

qPCR was used to determine viral titer and for biodistribution studies, as described.[17] The quantity of GFP target sequence in each sample was normalized to the quantity of the LaminB2 locus, with data expressed as double-stranded copies of GFP per two double-stranded copies of LaminB2. This approximates the copies of vector DNA per cell.

Animal procedures

All animals used in these studies were either male Sprague–Dawley rats (Charles River, Morrisville, NC, USA, 250–250 g) or adult female C57Bl/6 mice (Jackson Labs, Bar Harbor, ME, USA) that were maintained in a 12 h light–dark cycle and had free access to water and food. All care and procedures were in accordance with the National Institutes of Health Guide for the Care and Use of Laboratory Animals, and all procedures received prior approval by the University of North Carolina Institutional Animal Care and Use Committee.

6-hydroxy-dopamine treatment—Initially, rats ($N = 2$) were anesthetized with 50 mg kg^{-1} pentobarbital, intraperitoneal and placed into a stereotactic frame. Next, the rats received a unilateral infusion of 6-OHDA (2 μl, 20 μg μl^{-1}) into the right striatum (0.5 mm anterior to bregma, 3.5 mm lateral, 5.5 mm vertical, according to the atlas of Paxinos and Watson).[34] This treatment results in a significant reduction in striatal dopamine content 14 days posttreatment.

AAV capsid library administration—The AAV capsid library was administered 14 days post-6-OHDA treatment. For each selection round, two rats were anesthetized initially with pentobarbital (50 mg kg^{-1} intraperitoneal) and subsequently received an intravenous tail vein injection of the AAV capsid library virus (100 μl, 6.7×10^{12} vg ml^{-1}). Three days later, the rats were killed and the right striatum was dissected out. Subsequently, cells were mechanically dissociated as previously described[17] for subsequent PCR clone rescue.

Stereotactic AAV vector administration—As above, rats were anesthetized with pentobarbital and placed into a stereotactic frame. Olig001-CBh-GFP at a titer of 5.2×10^{12} vg ml^{-1} was infused at a rate of 1 µl per 5 min (5.2×10^9 vg over 5 min) into the striatum (0.5 mm anterior to bregma, 3.5 mm lateral, 5.5 mm vertical), according to the rat brain atlas of Paxinos and Watson.[34] The rats were killed for immunohistochemical evaluation 14 days post-vector infusion.

Immunohistochemistry—Fourteen days post-vector infusion, rats received an overdose of pentobarbital (100 mg kg^{-1}, intraperitoneal) and subsequently were perfused transcardially with 100 ml of ice-cold 0.1 M PBS pH 7.4 (25 ml min^{-1}), followed by 180 ml of ice-cold 4% paraformaldehyde-phosphate buffer (pH 7.4) (30 ml min^{-1}). Each brain was post-fixed in 4% paraformaldehyde-phosphate buffer (pH 7.4) overnight at 4 °C. Fixed brains were sectioned coronally on a Leica (Wetzlar, Germany) vibratome (40-µm thick) and stored in ice-cold 0.1 M PBS pH 7.4 until further processing. For immunostaining, slides were washed three times for 5 min in 0.1 M PBS pH 7.4, then blocked in 10% goat serum and 0.1% Triton-X in 0.1 M PBS pH 7.4 for 30 min. Primary antibodies NeuN (1:500; Millipore, Bedford, MA, USA; MAB377), Olig2 (1:250; Millipore; AB9610) and glial fibrillary acidic protein (1:2000; Dako (Glostrup, Denmark); Z0334) were incubated in 5% goat serum and 0.05% Triton-X in 0.1 M PBS pH 7.4 at 4 °C with gentle agitation overnight. Sections were washed in 0.1 M PBS pH 7.4 and blocked again as described above. Secondary goat anti-mouse Alexa 594 (A11032) was used for detection of NeuN or goat anti-rabbit Alexa 594 (A11080) was used for detection of glial fibrillary acidic protein and Olig2 (both 1:500 in 5% goat serum and 0.5% Triton-X in 0.1 M PBS pH 7.4 with gentle agitation at 4 °C for 45 min). Sections were washed with 0.1 M PBS pH 7.4 three times for 5 min each. Sections were floated, put on glass slides, and dried overnight at room temperature. Slides were then mounted with fluorescent mounting media and cover slipped. Confocal imaging was performed at the Michael Hooker Microscopy Core at UNC-Chapel Hill using a Leica Sp2 confocal. Slides were visualized using the oil 40× objective using sequential laser scanning to obtain z-stacks. Z-stacks were ~ 4 µm with 10–12 slices 0.36 µm thick per stack. Stacks were flattened in the Leica software and processed in Image J (NIH, Bethesda, MD, USA).

Biodistribution—Adult female C57Bl/6 mice (Jackson labs) were intravenously injected in the tail vein with 5×10^{10} vg (~2.5×10^{12} vg per kg body weight) in 200 µl PBS with 5% D-sorbitol. Ten days post injection organs were harvested. Total DNA from each organ was extracted with Qiagen DNeasy blood and tissue kit and total copies of GFP and mouse genomic LaminB2 were determined by qPCR. Data were compiled from five mice for AAV8 and four mice for Olig001. The s.e. of the mean was calculated.

In vitro binding

Mixed glial cultures were prepared from C57BL/6J day 3 neonatal pups.[35] Forebrains were minced, dissociated and washed prior to plating in T75 flasks. Cells were removed from the flasks and then replated into 35 mm tissue culture dishes with ~ 5×10^5 cells. At 95% confluency, Olig001 and AAV8 containing the CBh-GFP reporter genome were diluted and added separately, in quadruplicate, at a multiplicity of infection of 100 vg per cell and were

incubated at 4 °C with mixing every 10 min for 1 h. Plates were rinsed with ice-cold PBS three times, cells scraped from the plates, pelleted, and frozen at − 80 °C. A PBS only dish was also included as a mock sample. DNA was isolated from the samples using the Qiagen DNeasy blood and tissue kit. The amount of viral GFP and mouse genomic LaminB2 was determined by qPCR. Statistical analysis and graphing was done in Prism (GraphPad Software, La Jolla, CA, USA). Outliers were determined using the Grubbs test and subsequently removed. Statistical significance ($P < 0.05$) was determined using a one-tailed Mann–Whitney U-test. The fold change was determined using the average binding of each virus compared with average binding of AAV8. The errors bars on the fold difference graph were determined using percentages calculated from the binding data for each sample. To characterize the glial cell cultures, sister plates were provided glia media after the 1 h incubation at 4 °C with virus. The cultures were allowed to grow for 72 h at 37 °C. Cells were labeled with 10 μg ml^{-1} primary O4 antibody (MAB345, Millipore) followed by 5 μg ml^{-1} Alexa 594 (A21044, Invitrogen, Carlsbad, CA, USA) secondary antibody. Cells were fixed with 1% paraformaldehyde and stored at 4 °C until imaging. At least five independent fields were imaged on a Olympus IX71 inverted fluorescent microscope with cellSens Entry Software (Japan) and used for quantification of O4-positive cells in AAV8- and Olig001-treated plates.

Acknowledgments

References

1. Hadaczek P, Eberling JL, Pivirotto P, Bringas J, Forsayeth J, Bankiewicz KS. Eight years of clinical improvement in MPTP-lesioned primates after gene therapy with AAV2-hAADC. Mol Ther. 2010; 18:1458–1461. [PubMed: 20531394]

2. Kantor B, McCown T, Leone P, Gray SJ. Clinical applications involving CNS gene transfer. Adv Genet. 2014; 87:71–124. [PubMed: 25311921]

3. Kantor B, Bailey RM, Wimberly K, Kalburgi SN, Gray SJ. Methods for gene transfer to the central nervous system. Adv Genet. 2014; 87:125–197. [PubMed: 25311922]

4. McPhee SW, Janson CG, Li C, Samulski RJ, Camp AS, Francis J, et al. Immune responses to AAV in a phase I study for Canavan disease. J Gene Med. 2006; 8:577–588. [PubMed: 16532510]

5. Muramatsu S, Fujimoto K, Kato S, Mizukami H, Asari S, Ikeguchi K, et al. A phase I study of aromatic L-amino acid decarboxylase gene therapy for Parkinson's disease. Mol Ther. 2010; 18:1731–1735.

6. Rafii MS, Baumann TL, Bakay RA, Ostrove JM, Siffert J, Fleisher AS, et al. A phase1 study of stereotactic gene delivery of AAV2-NGF for Alzheimer's disease. Alzheimers Dement. 2014; 10:571–581. [PubMed: 24411134]

7. Burger C, Gorbatyuk OS, Velardo MJ, Peden CS, Williams P, Zolotukhin S, et al. Recombinant AAV viral vectors pseudotyped with viral capsids from serotypes 1, 2, and 5 display differential efficiency and cell tropism after delivery to different regions of the central nervous system. Mol Ther. 2004; 10:302–317. [PubMed: 15294177]

8. Davidson BL, Stein CS, Heth JA, Martins I, Kotin RM, Derksen TA, et al. Recombinant adeno-associated virus type 2, 4, and 5 vectors: transduction of variant cell types and regions in the mammalian central nervous system. Proc Natl Acad Sci USA. 2000; 97:3428–3432. [PubMed: 10688913]

9. Harding TC, Dickinson PJ, Roberts BN, Yendluri S, Gonzalez-Edick M, Lecouteur RA, et al. Enhanced gene transfer efficiency in the murine striatum and an orthotopic glioblastoma tumor model, using AAV-7- and AAV-8-pseudotyped vectors. Hum Gene Ther. 2006; 17:807–820. [PubMed: 16942441]

10. Klein RL, Dayton RD, Leidenheimer NJ, Jansen K, Golde TE, Zweig RM. Efficient neuronal gene transfer with AAV8 leads to neurotoxic levels of tau or green fluorescent proteins. Mol Ther. 2006; 13:517–527. [PubMed: 16325474]

11. Foust KD, Nurre E, Montgomery CL, Hernandez A, Chan CM, Kaspar BK. Intravascular AAV9 preferentially targets neonatal neurons and adult astrocytes. Nat Biotechnol. 2009; 27:59–65. [PubMed: 19098898]

12. Cearley CN, Wolfe JH. Transduction characteristics of adeno-associated virus vectors expressing cap serotypes 7, 8, 9, and Rh10 in the mouse brain. Mol Ther. 2006; 13:528–537. [PubMed: 16413228]

13. Cearley CN, Vandenberghe LH, Parente MK, Carnish ER, Wilson JM, Wolfe JH. Expanded repertoire of AAV vector serotypes mediate unique patterns of transduction in mouse brain. Mol Ther. 2008; 16:1710–1718. [PubMed: 18714307]

14. San Sebastian W, Samaranch L, Heller G, Kells AP, Bringas J, Pivirotto P, et al. Adeno-associated virus type 6 is retrogradely transported in the non-human primate brain. Gene Therapy. 2013; 20:1178–1183. [PubMed: 24067867]

15. Chen H, McCarty DM, Bruce AT, Suzuki K, Suzuki K. Gene transfer and expression in oligodendrocytes under the control of myelin basic protein transcriptional control region mediated by adeno-associated virus. Gene Therapy. 1998; 5:50–58. [PubMed: 9536264]

16. Lawlor PA, Bland RJ, Mouravlev A, Young D, During MJ. Efficient gene delivery and selective transduction of glial cells in the mammalian brain by AAV serotypes isolated from nonhuman primates. Mol Ther. 2009; 17:1692–1702. [PubMed: 19638961]

17. Gray SJ, Blake BL, Criswell HE, Nicolson SC, Samulski RJ, McCown TJ, et al. Directed evolution of a novel adeno-associated virus (AAV) vector that crosses the seizure-compromised blood-brain barrier (BBB). Mol Ther. 2010; 18:570–578. [PubMed: 20040913]

18. Agbandje-McKenna M, Kleinschmidt J. AAV capsid structure and cell interactions. Methods Mol Biol. 2011; 807:47–92. [PubMed: 22034026]

19. Govindasamy L, Padron E, McKenna R, Muzyczka N, Kaludov N, Chiorini JA, et al. Structurally mapping the diverse phenotype of adeno-associated virus serotype 4. J Virol. 2006; 80:11556–11570. [PubMed: 16971437]

20. Nonnenmacher M, Weber T. Intracellular transport of recombinant adeno-associated virus vectors. Gene Therapy. 2012; 19:649–658. [PubMed: 22357511]

21. Asokan A, Conway JC, Phillips JL, Li C, Hegge J, Sinnott R, et al. Reengineering a receptor footprint of adeno-associated virus enables selective and systemic gene transfer to muscle. Nat Biotechnol. 2010; 28:79–82. [PubMed: 20037580]

22. Bowles DE, McPhee SW, Li C, Gray SJ, Samulski JJ, Camp AS, et al. Phase 1 gene therapy for Duchenne muscular dystrophy using a translational optimized AAV vector. Mol Ther. 2012; 20:443–455. [PubMed: 22068425]

23. Pulicherla N, Shen S, Yadav S, Debbink K, Govindasamy L, Agbandje-McKenna M, et al. Engineering liver-detargeted AAV9 vectors for cardiac and musculoskeletal gene transfer. Mol Ther. 2011; 19:1070–1078. [PubMed: 21364538]

24. Hughes EG, Kang SH, Fukaya M, Bergles DE. Oligodendrocyte progenitors balance growth with self-repulsion to achieve homeostasis in the adult brain. Nat Neurosci. 2013; 16:668–676. [PubMed: 23624515]

25. Kang SH, Li Y, Fukaya M, Lorenzini I, Cleveland DW, Ostrow LW, et al. Degeneration and impaired regeneration of gray matter oligodendrocytes in amyotrophic lateral sclerosis. Nat Neurosci. 2013; 16:571–579. [PubMed: 23542689]

26. Gray SJ, Foti SB, Schwartz JW, Bachaboina L, Taylor-Blake B, Coleman J, et al. Optimizing promoters for recombinant adeno-associated virus-mediated gene expression in the peripheral and central nervous system using self-complementary vectors. Hum Gene Ther. 2011; 22:1143–1153. [PubMed: 21476867]

27. Sondhi D, Hackett NR, Peterson DA, Stratton J, Baad M, Travis KM, et al. Enhanced survival of the LINCL mouse following CLN2 gene transfer using the rh.10 rhesus macaque-derived adeno-associated virus vector. Mol Ther. 2007; 15:481–491. [PubMed: 17180118]

28. Taymans JM, Vandenberghe LH, Haute CV, Thiry I, Deroose CM, Mortelmans L, et al. Comparative analysis of adeno-associated viral vector serotypes 1, 2, 5, 7, and 8 in mouse brain. Hum Gene Ther. 2007; 18:195–206. [PubMed: 17343566]

29. Klein RL, Dayton RD, Tatom JB, Henderson KM, Henning PP. AAV8, 9, Rh10, Rh43 vector gene transfer in the rat brain: effects of serotype, promoter and purification method. Mol Ther. 2008; 16:89–96. [PubMed: 17955025]

30. Paneda A, Vanrell L, Mauleon I, Crettaz JS, Berraondo P, Timmermans EJ, et al. Effect of adeno-associated virus serotype and genomic structure on liver transduction and biodistribution in mice of both genders. Hum Gene Ther. 2009; 20:908–917. [PubMed: 19419275]

31. Xiao PJ, Li C, Neumann A, Samulski RJ. Quantitative 3D tracing of gene-delivery viral vectors in human cells and animal tissues. Mol Ther. 2012; 20:317–328. [PubMed: 22108857]

32. Li W, Asokan A, Wu Z, Van Dyke T, DiPrimio N, Johnson JS, et al. Engineering and selection of shuffled AAV genomes: a new strategy for producing targeted biological nanoparticles. Mol Ther. 2008; 16:1252–1260.

33. Gray SJ, Nagabhushan Kalburgi S, McCown TJ, Jude Samulski R. Global CNS gene delivery and evasion of anti-AAV-neutralizing antibodies by intrathecal AAV administration in non-human primates. Gene Therapy. 2013; 20:450–459. [PubMed: 23303281]

34. Paxinos, G., Watson, C. The Rat Brain in Stereotaxic Coordinates. Academic Press; San Diego, CA, USA: 2014.

35. McCarthy KD, de Vellis J. Preparation of separate astroglial and oligodendroglial cell cultures from rat cerebral tissue. J Cell Biol. 1980; 85:890–902. [PubMed: 6248568]
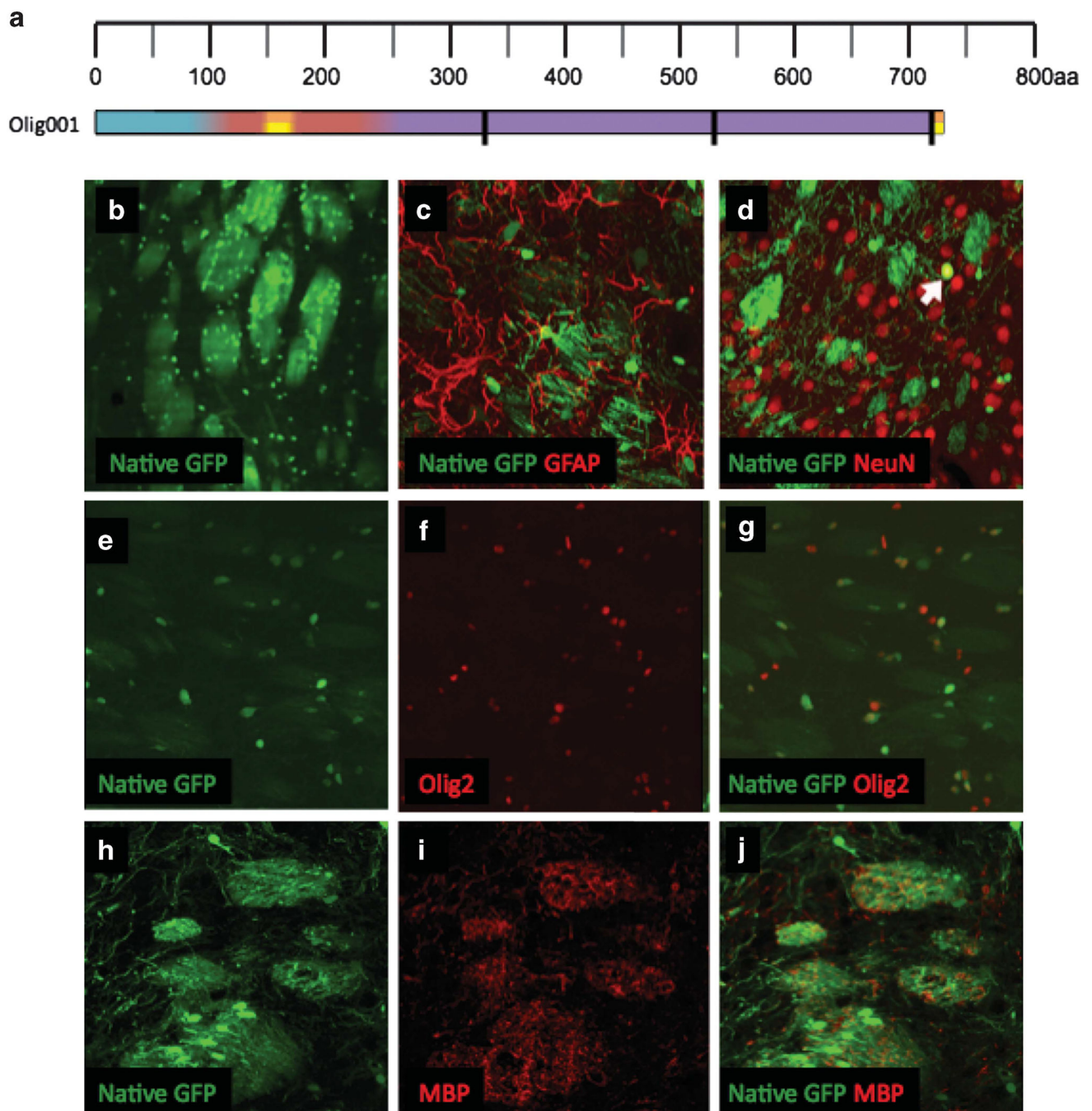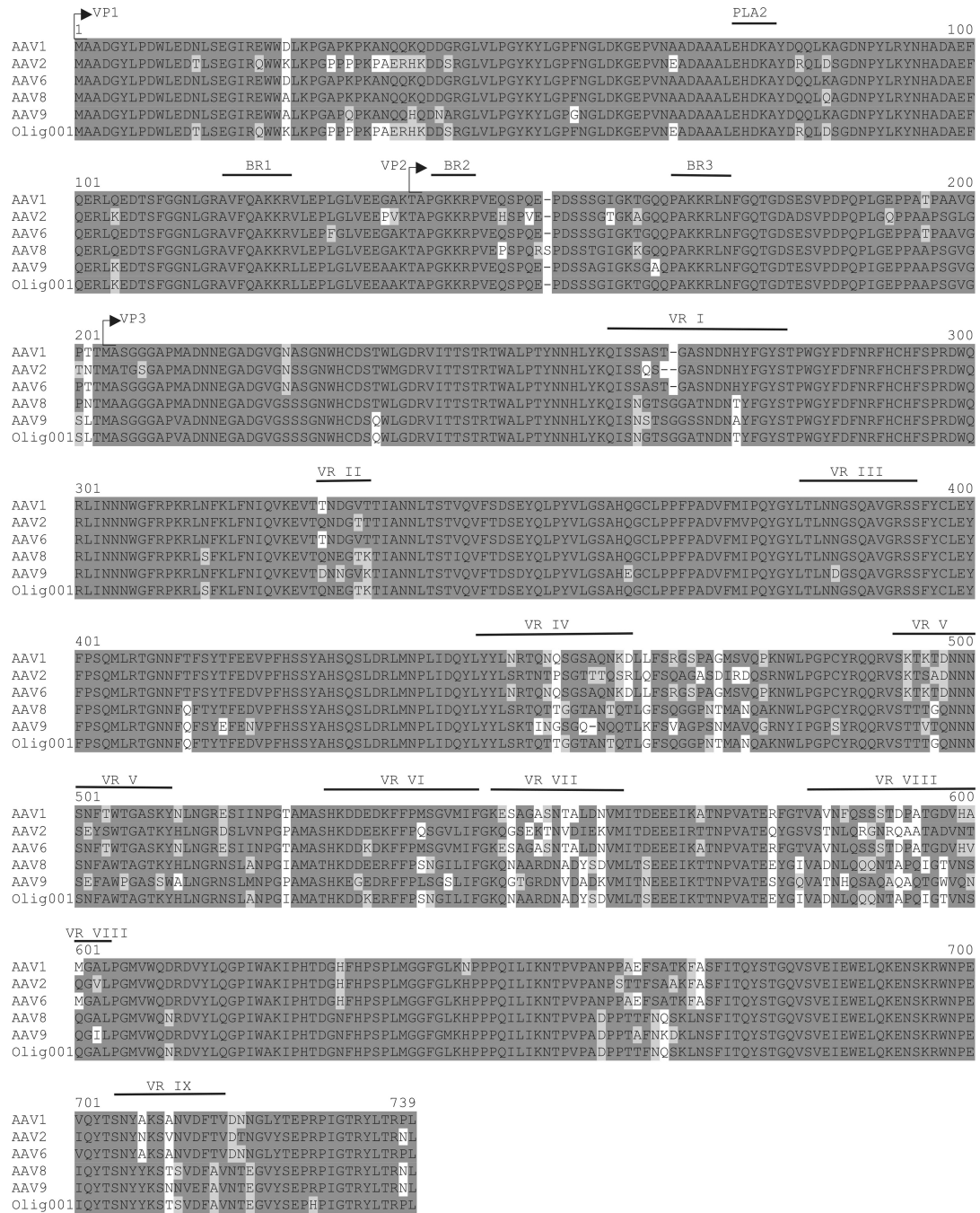
Figure 1.

Olig001 has an oligodendrocyte-preferring tropism. (**a**) Diagram of the *cap* gene from Olig001. Each color represents a different AAV parental serotype (blue = AAV2, purple = AAV8, red = AAV9, yellow = AAV1 and orange = AAV6) present in the input reaction of the library. The black vertical bars indicate point mutations. (**b–j**) Naïve rats were striatally infused with Olig001-CBh-GFP (5.2×10^9 vg over 5 min) and harvested 2 weeks later. (**b**) Confocal imaging shows Olig001 transduction of cells in the rat striatum that exhibit characteristics indicative of oligodendrocytes including the localization of GFP-positive

myelin in the patch of the striatal patch/matrix. (**c**) Confocal imaging reveals a lack of co-localization of the GFP-positive cells with astrocytes labeled with glial fibrillary acidic protein (GFAP) (red) within the striatum. (**d**) Confocal imaging illustrates that the vast majority of Olig001-transduced cells within the striatum do not co-localize with a marker of neurons, NeuN (red). However, the arrow indicates a single GFP-/NeuN-positive cell. (**e–g**) Confocal imaging demonstrates that GFP-positive cells and Olig2 (red) co-localize. (**h–j**) Confocal imaging demonstrates that GFP-positive patches co-localize with MBP (myelin basic protein) patches within the striatum.
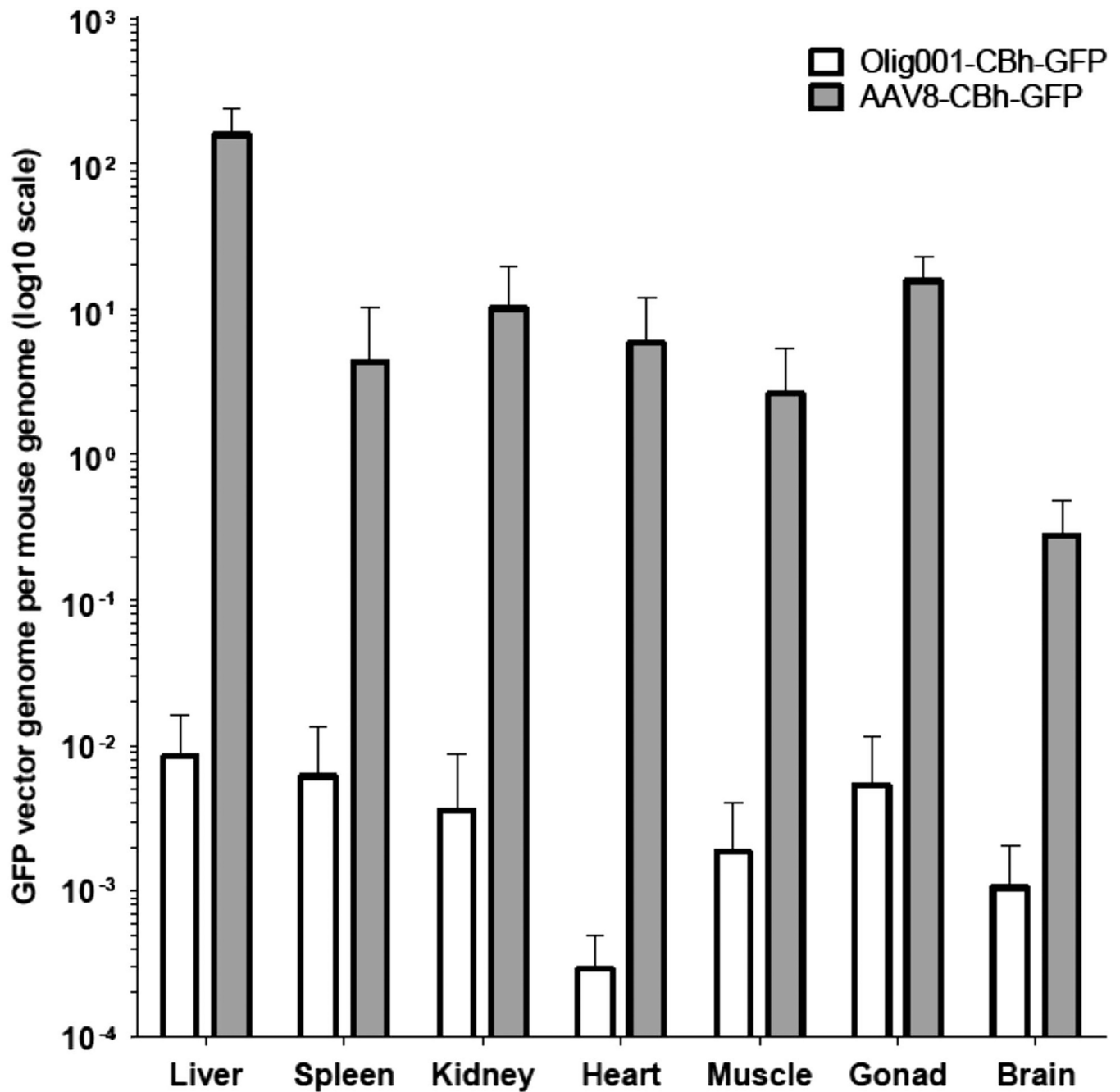
OLIG001 CAP>> 5'-
ATGGCTGCCGATGGTTATCTTCCAGATTGGCTCGAGGACACTCTCTCTGAAGGAATAAGACAGTGGTGGAAGCTCAA
ACCTGGCCCACCACCACCAAAGCCCGCAGAGCGGCATAAGGACGACAGCAGGGGTCTTGTGCTTCCTGGGTACAAG
TACCTCGGACCCTTCAACGGACTCGACAAGGGAGAGCCGGTCAACGAGGCAGACGCCGCGGCCCTCGAGCACGAC
AAAGCCTACGACCGGCAGCTCGACAGCGGAGACAACCCGTACCTCAAGTACAACCACGCCGACGCGGAGTTTCAGG
AGCGCCTTAAAGAAGATACGTCTTTTGGGGGCAACCTCGGGCGAGCAGTCTTCCAGGCCAAAAAGAGGCTTCTTGAA
CCTCTTGGTCTGGTTGAGGAAGCGGCTAAGACGGCTCCTGGAAAGAAGAGGCCTGTAGAGCAGTCTCCTCAGGAAC
CGGACTCCTCCTCGGGCATCGGCAAGACAGGCCAGCAGCCCGCTAAAAAGAGACTCAATTTCGGTCAGACTGGCGA
CACAGAGTCAGTCCCAGACCCTCAACCAATCGGAGAACCTCCCGCAGCCCCCTCAGGTGTGGGATCTCTTACAATG
GCTTCAGGTGGTGGCGCACCAGTGGCAGACAATAACGAAGGTGCCGATGGAGTGGGTAGTTCCTCGGGAAATTGGC
ATTGCGATTCCCAATGGCTGGGGGACAGAGTCATCACCACCAGCACCCGAACCTGGGCCCTGCCCACCTACAACAA
TCACCTCTACAAGCAAATCTCCAACGGGACATCGGGAGGAGCCACCAACGACAACACCTACTTCGGCTACAGCACCC
CCTGGGGGTATTTTGACTTTAACAGATTCCACTGCCACTTTTCACCACGTGACTGGCAGCGACTCATCAACAACAACT
GGGGATTCCGGCCCAAGAGACTCAGCTTCAAGCTCTTCAACATCCAGGTCAAGGAGGTCACGCAGAATGAAGGCAC
CAAGACCATCGCCAATAACCTTACCAGCACGGTCCAGGTCTTCACGGACTCGGAGTACCAGCTGCCGTACGTTCTCG
GCTCTGCCCACCAGGGCTGCCTGCCTCCGTTCCCGGCGGACGTGTTCATGATTCCCCAGTACGGCTACCTAACACT
CAACAACGGTAGTCAGGCCGTGGGACGCTCCTCCTTCTACTGCCTGGAATACTTTCCTTCGCAGATGCTGAGAACCG
GCAACAACTTCCAGTTTACTTACACCTTCGAGGACGTGCCTTTCCACAGCAGCTACGCCCACAGCCAGAGCTTGGAC
CGGCTGATGAATCCTCTGATTGACCAGTACCTGTACTACTTGTCTCGGACTCAAACAACAGGAGGCACGGCAAATAC
GCAGACTCTGGGCTTCAGCCAAGGTGGGCCTAATACAATGGCCAATCAGGCAAAGAACTGGCTGCCAGGACCCTGT
TACCGCCAACAACGCGTCTCAACGACAACCGGGCAAAACAACAATAGCAACTTTGCCTGGACTGCTGGGACCAAATA
CCATCTGAATGGAAGAAATTCATTGGCTAATCCTGGCATCGCTATGGCAACACACAAAGACGACAAGGAGCGTTTTTT
TCCCAGTAACGGGATCCTGATTTTTGGCAAACAAATGCTGCCAGAGACAATGCGGATTACAGCGATGTCATGCTCA
CCAGCGAGGAAGAAATCAAAACCACTAACCCTGTGGCTACAGAGGAATACGGTATCGTGGCAGATAACTTGCAGCAG
CAAAACACGGCTCCTCAAATTGGAACTGTCAACAGCCAGGGGGCCTTACCCGGTATGGTTTGGCAGAACCGGGACG
TGTACCTGCAGGGTCCCATCTGGGCCAAGATTCCTCACACGGACGGCAACTTCCACCCGTCTCCGCTGATGGGCGG
CTTTGGCCTGAAACATCCTCCGCCTCAGATCCTGATCAAGAACACGCCTGTACCTGCGGATCCTCCGACCACCTTCA
ACCAGTCAAAGCTGAACTCTTTCATCACGCAATACAGCACCGGACAGGTCAGCGTGGAAATTGAATGGGAGCTGCAG
AAGGAAAACAGCAAGCGCTGGAACCCCGAGATCCAGTACACCTCCAACTACTACAAATCTACAAGTGTGGACTTTGC
TGTTAATACAGAAGGCGTGTACTCTGAACCCCACCCCATTGGCACCCGTTACCTCACCCGTCCCCTGTAA-3'

Figure 2.
DNA sequence of the *cap* gene of Olig001.

Figure 3.
Multiple protein alignment of Olig001 and parental serotypes (AAV1, 2, 6, 8 and 9) *cap* genes. Residues that are dark gray shaded are identical, light gray shaded are similar and white shaded are non-similar. The start sites for VP1, VP2 and VP3 are indicated. Regions that are required for transduction in VP1 and VP2 are indicated. Variable loops regions (VR) are indicated.

Figure 4.
Olig001 is detargeted from peripheral tissues compared with AAV8. Adult female C57Bl/6 mice received an intravenous dose of 5×10^{10} vg (~2.5×10^{12} vg per kg body weight) of either Olig001-CBh-GFP (white bars; $n = 4$) or AAV8-CBh-GFP (gray bars; $n = 5$). Ten days later the organ distribution of GFP genome per diploid mouse genome (LaminB2) was determined by qPCR. Error bars indicate s.e. of the mean.
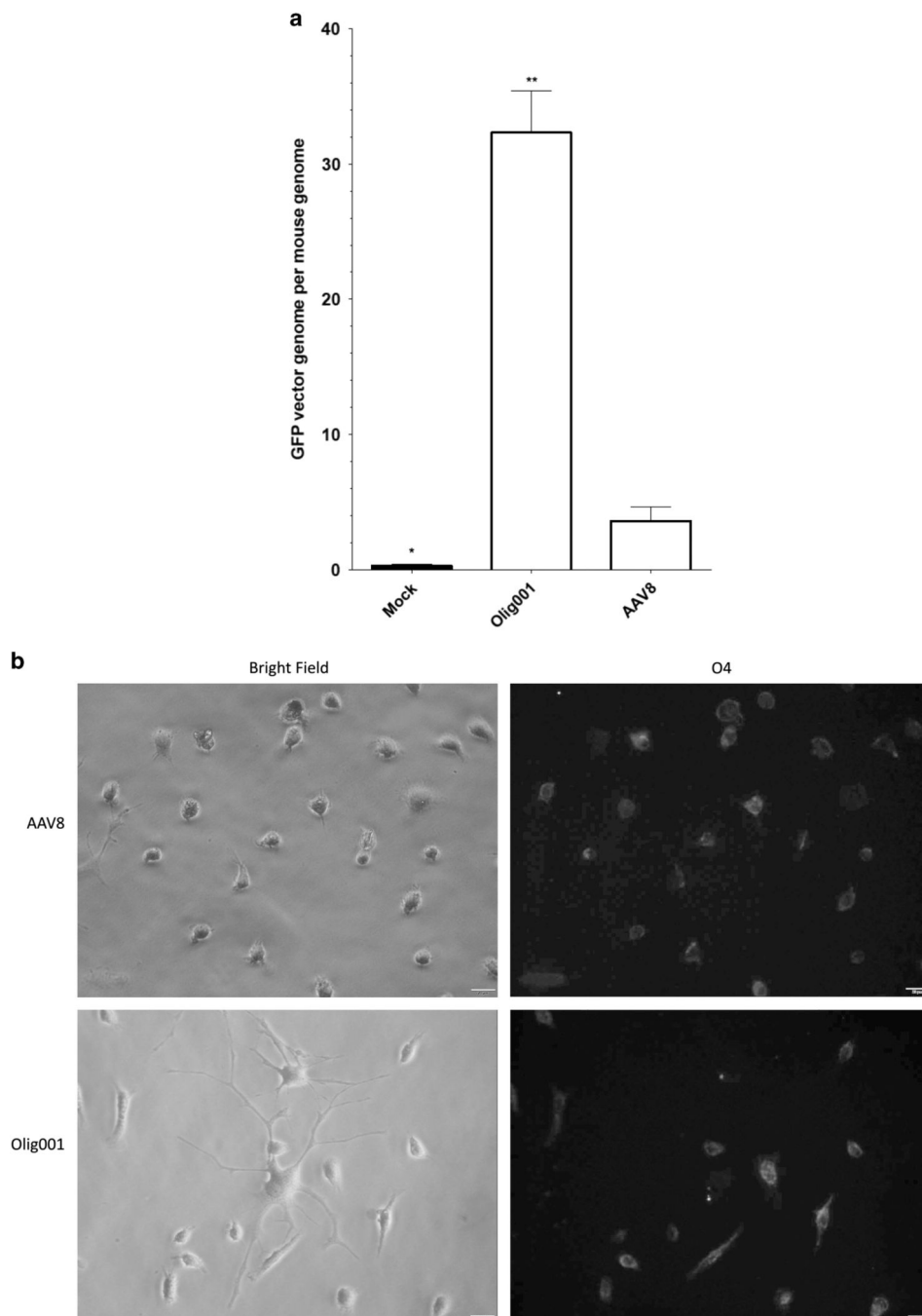
Figure 5.
In vitro binding analysis agrees with *in vivo* tropism. *In vitro*-mixed glial cell cultures were created by dissociating neonatal day 3 mouse brains. Plates containing ~ 5×10^5 cells were incubated with an multiplicity of infection of 100 vg per cell of AAV8-CBh-GFP, Olig001-CBh-GFP or PBS only for 1 h at 4 °C to allow for vector binding, but not uptake. (**a**) The amount of vector bound to cells was quantified by qPCR for GFP and normalized to mouse genomic LaminB2. Error bars indicate s.e. of the mean, * indicates a significant difference of $P < 0.03$ and ** indicates a significant difference of $P < 0.01$ compared with AAV8. The

errors bars were determined using percentages calculated from the binding data for each sample. (**b**) Sister cultures treated with AAV8 and Olig001, as described above, were incubated at 37 °C for 72 h. After 72 h cells were stained for an oligodendrocyte marker, O4, to determine how enriched the mixed glial cultures were for oligodendrocytes. At least five fields were imaged in bright field and fluorescence for quantification; 89% of AAV8- and 86% of Olig001-treated cells were O4-positive.